



15th Global Conference on Sustainable Manufacturing

Development of a Model for Predicting Cycle Time in Hot Stamping

R Muvunzi^{a*}, DM Dimitrov^a, S Matope^a, TM Harms^b

^aDepartment of Industrial Engineering, Faculty of Engineering, Stellenbosch University

^bDepartment of Mechanical and Mechatronic Engineering, Faculty of Engineering, Stellenbosch University, Stellenbosch 7600, South Africa

Abstract

In manufacturing, reducing the cycle time results in lower production costs. The cycle time in a hot stamping process affects the quality characteristics (tensile strength) of formed parts. A faster cooling rate (>27 K/s) of the blank guarantees the production of a part with the required microstructural properties (martensite). This compels researchers to continuously develop ways of increasing the manufacturing speed. On the other hand, it is important to predict the minimum cycle time for a given set of parameters which does not compromise the quality of formed parts. In this paper, a model for predicting the cycle time for a hot stamping process is presented. The lumped heat capacitance method is used in formulating the model since the temperature gradient across the blank and heat transfer within the plane of the blank are considered negligible. To validate the equation, a finite element simulation was conducted using Pam-Stamp software. The results show that the proposed model can be useful in further studies targeted towards cycle time reduction in hot sheet metal forming processes.

© 2018 The Authors. Published by Elsevier B.V.

Peer-review under responsibility of the scientific committee of the 15th Global Conference on Sustainable Manufacturing (GCSM).

Keywords: hot stamping; cycle time; model; blank

1 Introduction

In hot stamping, a thin metal sheet (blank) is heated to a high temperature (between 900 to 950 °C) and transferred to a press where it is formed and quenched. This results in the production of components with high tensile strength

* Corresponding author. Tel.: +27633955078.

E-mail address: rmuvunzi@sun.ac.za

(1500 MPa) [1]. Figure 1 summarizes the hot stamping process.

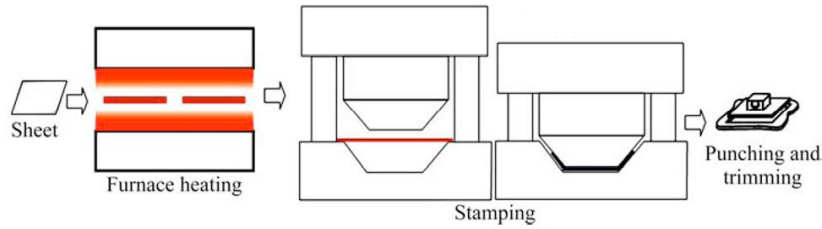


Figure 1: Hot stamping process [2]

The cooling stage occupies more than 30 % of the total cycle time [3]. Hot stamping tools are manufactured with an in-built cooling system in the form of channels in which a coolant flows to extract heat from the tool. An increase in the cooling rate results in improved productivity. Research efforts are targeted towards the reduction of the cycle time. This involves design of more effective cooling systems with improved heat transfer capabilities. Shan *et al.* [4] suggested a method for calculating optimum cooling system parameters based on theoretical analysis and numerical simulation. Lim *et al.* [5] proposed two approaches for designing cooling systems. The first approach is focused on reducing maintenance costs and the other is centred on the reduction of cycle time. A reduction of cycle time by 25 % was achieved. Liu *et al.* [6] used the evolutionary algorithm to design a hot stamping tool with optimized cooling channels and this resulted in a cooling rate of 40 °C/s. Lin *et al.* [7] developed another method based on simulation.

Another strategy for reducing the cooling time involves the use of tool steels with improved thermal conductivity [8]. Ghiotti *et al.* [9] investigated the application new tool steels with thermal conductivity of up to 60 W/m°C. Further information on the use of high thermal conductivity tool steels (30-45 W/mK) was presented by Escher and Wilzer [10]. Despite all the above-mentioned efforts, there has not been much study focused on determining the minimum cycle time. It is important to identify the minimum possible cycle time which does not compromise the quality of parts as this will be used in further research as a benchmark for seeking opportunities for further reducing the cycle time. The paper presents a model which was developed to predict the minimum cycle time in hot stamping. The cycle time is considered as the total time for transfer, forming, cooling and extraction of the blank.

In developing the model, the thermal gradient across the blank is assumed to be negligible because of the small blank thickness (0.6-3.0 mm), high thermal conductivity (40-45 W/mK) and large surface area to volume ratio of the blank [11]. Hence, the lumped heat capacity method was considered since it is applicable for situations when the thermal gradient is negligible. Abdulhay *et al.* [11] calculated the Biot number using a blank with a thickness of 1.55 mm at different contact pressure values (0-30 MPa). Although the range for the Biot number obtained from the calculations varied between 0.05 and 0.25, they considered the blank as having uniform temperature. According to experiments conducted by Zhao *et al.* [12] using a 2 mm blank, the maximum Biot number was 0.2. Similarly, the temperature gradient across the blank is assumed to be negligible. For situations in which there is significant thermal gradient in a solid, the finite difference method becomes applicable. External heat transfer modes might include convection (q_{conv}), radiation (q_{rad}), surface heat flux (q) and internal heat energy generation (\dot{E}_g) [13]. The general lumped capacitance analysis can be summarized using equation 1 as stated by Bergman *et al.* [13].

$$q + \dot{E}_g - (q_{conv} + q_{rad}) = \dot{E} \quad (1)$$

The lumped heat capacitance method has been applied for the transfer and cooling time. In this case, the total cycle time is regarded as the sum of transfer (t_1), placement, extraction (t_2) and cooling time (t_3) as shown in equation 2.

$$t_c = t_1 + t_2 + t_3 \quad (2)$$

Nomenclature

A_b	Cross sectional area of blank (m^2)
A_d	Cross sectional area of tool in contact with blank (m^2)
a	Material constant
C_v	Specific heat capacity at constant volume ($\text{J/kg}^\circ\text{C}$)
e_s	Ejector stroke (mm)
\dot{E}	Rate of change in internal heat energy (W)
\dot{E}_g	Rate of internal heat energy generation (W)
l_s	Punch stroke (mm)
n	Material constant
q	Surface heat flux (W)
q_{conv}	Convection heat transfer (W)
q_{rad}	Radiation heat transfer (W)
h_c	Interfacial heat transfer coefficient ($\text{W/m}^2\text{C}$)
s	Blank thickness (mm)
t	Time (s)
T_b	Temperature of blank ($^\circ\text{C}$)
T_{bi}	Initial temperature of blank in the transfer stage ($^\circ\text{C}$)
T_{bo}	Initial temperature of blank in the cooling stage ($^\circ\text{C}$)
T_d	Temperature of tool ($^\circ\text{C}$)
T_{fac}	Temperature of floor and surrounding facilities ($^\circ\text{C}$)
V	Volume of blank (m^3)
v_p	Velocity of punch (mm/s)
v_e	Velocity of ejector (mm/s)
ε	Emissivity -
ρ	Density (kg/m^3)
σ	Stefan Boltzmann constant ($\text{Wm}^{-2}\text{C}^{-4}$)

2 Model development

2.1 General considerations

The minimum transfer time (t_1) of the blank depends on the mechanical capability of the transfer system. The system can be in the form of a conveyor belt or robotic arms. In such cases, the speed of the material handling devices plays a major role. However, if a temperature change is required, the transfer time can be calculated using heat transfer principles.

During the time that the blank is transferred from furnace to the stamping tool, it loses heat by radiation and convection to the surrounding air at atmospheric temperature [14, 15]. Figure 2 illustrates the transfer stage.

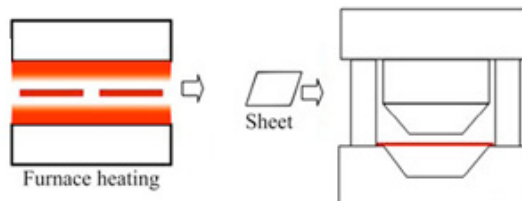


Figure 2: Transfer phase in hot stamping [2]

It is assumed that the blank is transferred in a horizontal position so that a constant height is maintained for easier positioning on the press. Shapiro *et al.* [15] revealed that radiation heat loss far exceeds the convection by up to ten

times. Hence, the effect of convection is neglected. The radiation heat lost by the blank on both sides is shown in equation 3.

$$q_{rad} = -2\sigma\epsilon A_b(T_b^4 - T_{fac}^4) \quad (3)$$

Equation 4 represents the rate of change in internal heat energy of the blank based on the assumption that a specific heat (c_v) is used.

$$\dot{E} = \rho c_v V \frac{dT}{dt} \quad (4)$$

There is no applied surface heat flux or internal energy generation during the transfer phase. Thus substituting equations 3 and 4 into 1 results in the following expression [15].

$$\rho c_v V \frac{dT}{dt} = -2\sigma\epsilon A_b(T_b^4 - T_{fac}^4) \quad (5)$$

Solving equation 5 and making t the subject results in

$$t_1 = \frac{\rho c_v V}{8\sigma\epsilon A_b T_b^3} \left\{ \ln \frac{(T_{fac} + T_b)/(T_b - T_{fac})}{(T_{fac} + T_{b_i})/(T_{b_i} - T_{fac})} + 4 \left[\tan \left(\frac{T_b}{T_{fac}} \right) - \tan^{-1} \left(\frac{T_{b_i}}{T_{fac}} \right) \right] \right\} \quad (6)$$

Equation 6 is applicable when the initial and final blank temperature (T_b) values are known. Shapiro *et al.* [15] validated the equation and obtained a transfer time of 6.6 seconds which was close to the actual time (6.5 seconds).

2.2 Blank placement and extraction

During the placement phase, the punch moves down before forming takes place. The time taken for the punch to move depends on the possible maximum punch velocity and the stroke length. The punch velocity is governed by the material properties and product quality characteristics required. According to Todd [16], the time for punch movement and extraction can be obtained using equation 7.

$$t_2 = \frac{l_s}{v_p} + \frac{e_s}{v_e} \quad (7)$$

Regarding equation 7, the first expression represents the time that the punch moves down to conduct the forming operation. The second expression represents the time taken to extract the part after the forming operation.

2.3 Cooling time of blank in closed tools

The heat lost by the blank is transferred to the thermally controlled tools depending on the interfacial or contact heat transfer coefficient (h_c) as shown in Figure 3.

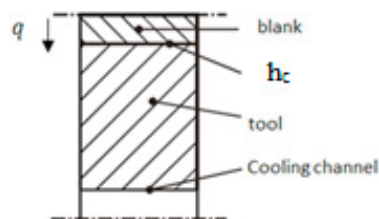


Figure 3: Heat loss from blank

As exposed in the figure, heat is transferred because of the contact between the surfaces. Equation 8 shows the heat flux by conduction from the blank to the punch and die surface [12], [17].

$$q = h_c A_b (T_b - T_d) \quad (8)$$

Most experimental results have proved that contact pressure has a great effect on h_c [18, 20]. Since the blank is held between closed tools, the effect of radiation and convection is considered negligible [14]. Thus, equation 8 is substituted into 1 as shown.

$$\rho c_v V \frac{dT}{dt} = -h_c A_b (T_b - T_d) \quad (9)$$

There is a negative sign on the right side of the equation since heat is being lost from the blank. Thus, there is a decrease in the internal heat energy of the blank. Solving the differential equation results in

$$T_{b(t)} - T_d = C e^{-\frac{h_c A_b t}{\rho c_v V}} \quad (10)$$

Substitution is done at initial conditions when t_3 is zero to obtain the value of C.

$$T_{b(t)} = (T_{b_0} - T_d) e^{-\frac{h_c A_b t_3}{\rho c_v V}} + T_d \quad (11)$$

Making t_3 the subject of the equation results in

$$t_3 = \frac{\rho c_v V}{h_c} \ln \frac{(T_{b_0} - T_d)}{(T_{b(t)} - T_d)} \quad (12)$$

Thus, the cooling time of the blank can be estimated using equation 12 given an initial blank temperature T_{b_0} . The initial temperature of the blank (T_{b_0}) will account for any heat generated within the blank due to friction and bending work.

The internal energy generated during forming imposes significant temperature gradients within the plane of the blank. However, the amount of heat transferred within the plane of the blank will be small due to the small cross-sectional area of the blank. Secondly, the key assumption is that the tool temperature (T_d) will remain uniform due to its internal cooling efficiency, rapidly removing any temperature differences. Thirdly, the lumped heat capacity approach for the blank implies that transients are not really of interest, a minimum time is sought.

3 FE Simulation

To test the validity of equation 12, a finite element simulation was conducted. Pam-Stamp software is considered for the analysis because it allows simulation of cooling time in hot sheet metal forming processes [21]. A simple part shown in Figure 4 was considered for the analysis. The blank material used in the analysis is boron-alloyed steel (22MnB5) because of its wide application in hot stamping parts. The length, width and thickness of the unfolded blank are 200, 150 and 2 mm respectively.

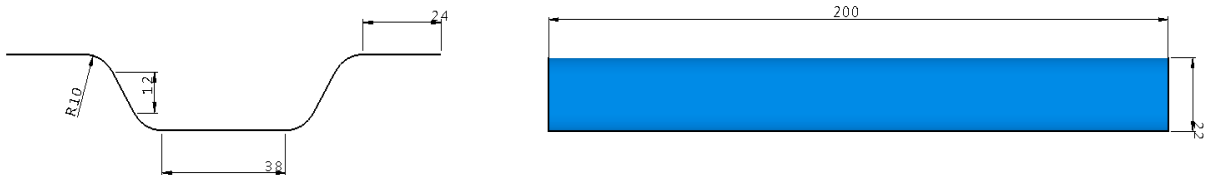


Figure 4: Dimensions of a simple part

The parameters required by the Pam-Stamp code used in the simulation are listed in Table 1.

Table 1. Simulation Parameters

Parameter	Description
Press type	Single action
Environmental temperature	25 °C
Start temperature of blank	810 °C
Stamping speed	50 mm/s
Cooling time (t_3)	(0-20 s)
Macro	HF Validation single action
Initial temperature of punch and die (T_d)	70 °C
Blank material	22MnB5
Density of blank (ρ)	7830 kg/m ³
Specific heat capacity of blank (c_v)	650 J/kg ⁰ C
Interfacial heat transfer coefficient (h_c)	Function of gap and pressure
Solver type	Shared memory processor

According to the simulation set up, the die moves to conduct the forming operation until the blank attains the desired shape while punch is fixed. This is followed by the cooling stage of the blank because of contact with the cold punch and die.

4 Results and discussion

The temperature profile of the blank after every two seconds is displayed in the form of colour maps as part of the simulation results. To summarize the results, Figure 5 shows the maximum and minimum temperature after every 4 seconds. Time intervals of 2 seconds were used in the analysis to capture more information on the temperature behaviour of the blank.

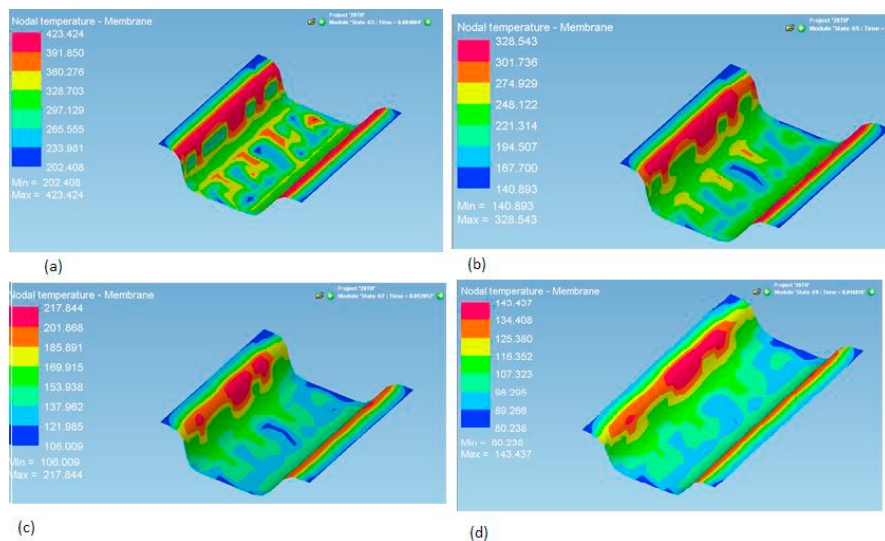


Figure 5: Temperature profile of blank after (a) 4 seconds (b) 8 seconds (c) 12 seconds (d) 16 seconds

Equation 12 is used to calculate the cooling time based on the maximum temperature values in Figure 5. In the calculations, the interfacial heat transfer coefficient is considered as a function of pressure in accordance with equation

13, where a (0.00084) and n (-0.0614) depend on the blank material (boron-alloyed steel) [11].

$$\frac{1}{R} = aP^n \quad (13)$$

The calculated values for the cooling time are then compared with the simulated values to make a comparison as shown in Figure 6. A similar trend for the simulation curve was reported by Zhao *et al.*[12].

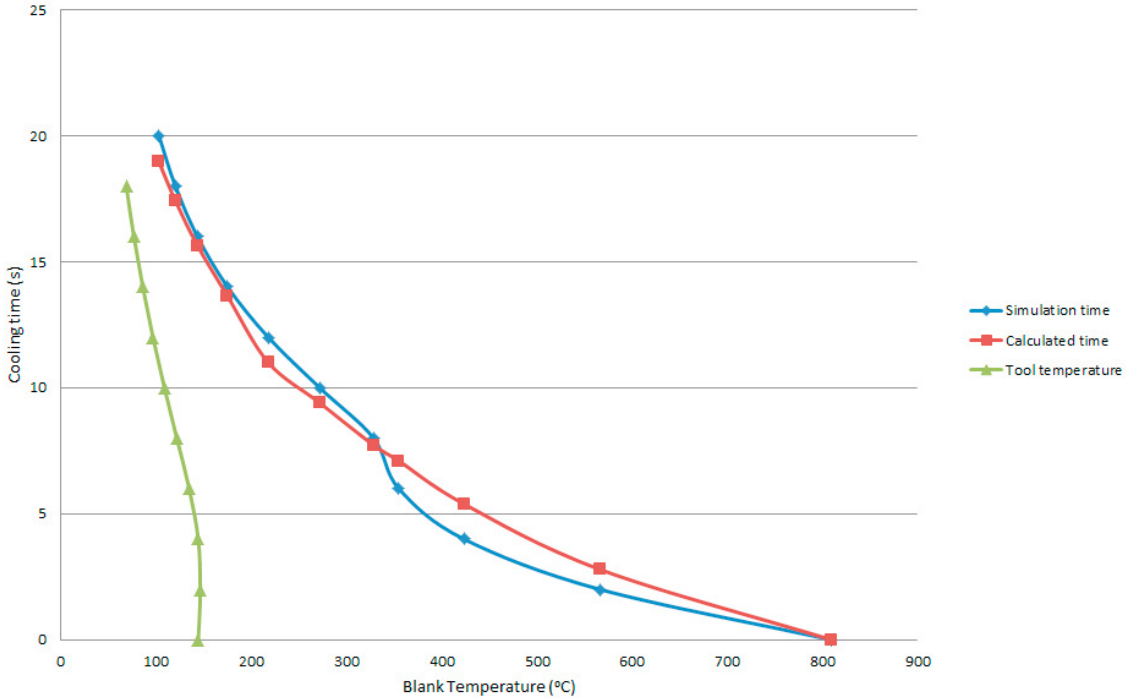


Figure 6: Graph showing change of temperature with time

The graph in Figure 6 shows a deviation between the simulated and calculated time values at the beginning of the process. It might be caused by the rapid heat loss of the blank due to the large temperature difference with the cold tools at the start of the process. Towards the end of the process, the calculated time values agree with the simulated maximum values.

In this single event, the punch and die will heat up absorbing the forming heat. However, this change in punch and die temperature (T_d) is small due to its large thermal mass. Figure 5 also reveals the expected long-term temperature trend for the blank to reach a uniform single temperature. Hence, equation 12 is useful in predicting the cooling time of the blank although there is need for further investigations using different materials. Thus, the total time can be calculated by substituting equations 6, 7 and 12 into 2 as shown below.

$$t_c = \frac{\rho c_v V}{8\sigma \epsilon A_b T_b^3} \left\{ \ln \frac{(T_{fac} + T_b)/(T_b - T_{fac})}{(T_{fac} + T_{b_i})/(T_{b_i} - T_{fac})} + 4 \left[\tan \left(\frac{T_b}{T_{fac}} \right) - \tan^{-1} \left(\frac{T_{b_i}}{T_{fac}} \right) \right] \right\} + \frac{l_s}{v_p} + \frac{e_s}{v_e} + \frac{\rho c_v S}{h_c} \ln \frac{(T_{b_o} - T_d)}{(T_{b(t)} - T_d)} \quad (14)$$

5 Conclusion

The aim of the paper was to present a model for predicting the cycle time in a hot stamping process. An equation for the cooling time of the blank was developed and validated using finite element analysis simulation. The next phase of this research will involve conducting physical experiments to validate the results from the simulation. Building up on previous studies, this has mapped the way forward in proposing the model for defining the total cycle time as stated

in equation 2 or 14 respectively. Further studies involve the experimental validation of the total cycle time equation.

Acknowledgements

The authors would like to thank the Organization for Women in Science for the Developing World (OWSD) and the Schlumberger Foundation for providing the financial resources to conduct the research. The paper is part of the PhD study of Ms Rumbidzai Muvunzi.

References

- [1] H. Karbasian and A. E. Tekkaya, "A review on hot stamping," *Journal of Materials. Processing Technology.*, vol. 210, no. 15, pp. 2103–2118, 2010.
- [2] K. Mori, "Smart hot stamping for ultra-high strength steel parts," in *60 Excellent Inventions in Metal Forming*, pp. 403–408, 2015.
- [3] B. Mueller, R. Hund, R. Malek, M. Gebauer, S. Polster, M. Kotzian, P. and R. Neugebauer "Added value in tooling for sheet metal forming through additive manufacturing," in *International Conference on Competitive Manufacturing*, pp. 51–58, 2013
- [4] Z. Shan, Y. S. Ye, M. L. Zhang, and B. Y. Wang, "Hot-stamping die-cooling system for vehicle door beams," *International Journal of Precision Engineering and Manufacturing*, vol. 14, no. 7, pp. 1251–1255, 2013.
- [5] W. S. Lim, H. S. Choi, S. Y. Ahn, and B. M. Kim, "Cooling channel design of hot stamping tools for uniform high-strength components in hot stamping process," *International Journal of Advanced Manufacturing Technology*, vol. 70, no. 5–8, pp. 1189–1203, 2014.
- [6] H. Liu, C. Lei, and Z. Xing, "Cooling system of hot stamping of quenched steel BR1500HS: Optimization and manufacturing methods," *International Journal of Advanced Manufacturing Technology.*, vol. 69, no. 1–4, pp. 211–223, 2013.
- [7] T. Lin, H. W. Song, S. H. Zhang, M. Cheng, and W. J. Liu, "Cooling systems design in hot stamping tools by a thermal-fluid-mechanical coupled approach," *Advances in Mechanical Engineering*, vol. 214, 2014.
- [8] T. Altan and A. E. Tekkaya, *Sheet metal Forming Processes and Applications*. ASTM International, 2012.
- [9] A. Ghiotti, S. Bruschi, F. Medea, and A. Hamasaiid, "Tribological behavior of high thermal conductivity steels for hot stamping tools," *Tribology International.*, vol. 97, pp. 412–422, 2016.
- [10] C. Escher and J. J. Wilzer, "Tool steels for hot stamping of high strength automotive body parts," *International Conference on Stone and Concrete Machining.*, vol. 3, pp. 219–228, 2015.
- [11] B. Abdulhay, B. Bourouga, C. Dessain, G. Brun, and J. Wilsius, "Development of estimation procedure of contact heat transfer coefficient at the part–tool interface in hot stamping process," *Heat Transfer Engineering*, vol. 32, no. 6, pp. 497–505, 2011.
- [12] K. Zhao, B. Wang, Y. Chang, X. Tang, and J. Yan, "Comparison of the methods for calculating the interfacial heat transfer coefficient in hot stamping," *Applied Thermal Engineering*, vol. 79, pp. 17–26, 2015.
- [13] T. L. Bergman, A. S. Lavigne, F. P. Incropera, and D. P. Dewitt, *Fundamentals of Heat and Mass Transfer*. 2011.
- [14] B. Abdulhay, B. Bourouga, and C. Dessain, "Experimental and theoretical study of thermal aspects of the hot stamping process," *Applied Thermal Engineering.*, vol. 31, no. 5, pp. 674–685, 2011.
- [15] A. B. Shapiro, "Using LS-Dyna for Hot Stamping," *7th European LS-DYNA Users Conference* no. 2, 2009.
- [16] R. H. Todd, D. K. Allen, and L. Alting, *Manufacturing processes reference guide*, First Edit. New York: Industrial Press Inc, 1994.
- [17] K. Ji, O. El Fakir, H. Gao, and L. Wang, "Determination of heat transfer coefficient for hot stamping Process," *Materials Today*, vol. 2, pp. S434–S439, 2015.
- [18] T.-H. Hung, P.-W. Tsai, F.-K. Chen, T.-B. Huang, and W.-L. Liu, "Measurement of Heat Transfer Coefficient of Boron Steel in Hot Stamping," *Procedia Engineering.*, vol. 81, no. October, pp. 1750–1755, 2014.
- [19] Q. Bai, J. Lin, L. Zhan, T. A. Dean, D. S. Balint, and Z. Zhang, "An efficient closed-form method for determining interfacial heat transfer coefficient in metal forming," *International Journal of Machine Tools and Manufacture*, vol. 56, pp. 102–110, 2012.
- [20] P. Bosetti, S. Bruschi, T. Stoehr, J. Lechler, and M. Merklein, "Interlaboratory comparison for heat transfer coefficient identification in hot stamping of high strength steels," *International Journal of Material Forming.*, vol. 3, no. SUPPL. 1, pp. 817–820, 2010.
- [21] ESI, "Pam_stamp Simulation Software." [Online]. Available: <https://www.esi-group.com/software-solutions/virtual-manufacturing/sheet-metal-forming/pam-stamp-stamping-simulation-solution>. [Accessed: 01-Apr-2017].